NASA Technical Memorandum 80192

SOME EXPERIENCE WITH ARC-HEATER SIMULATION

OF OUTER PLANET ENTRY RADIATION

W. L. Wells and W. L. Snow

January 1980

SOME EXPERIENCE WITH ARC-HEATER SIMULATION
OF OUTER PLANET ENTRY RADIATION

W. L. Wells and W. L. Snow
Langley Research Center

SUMMARY

A 55-cm long, 2.4-cm diameter, wall-stabilized arc heater was operated with pure hydrogen, pure helium, and two mixtures of hydrogen and helium. The heater was operated with 800 A and at 10^5 Pa (1 atm). From an end view of the arc, the spectra were measured over the 130- to 850-nm wavelength interval for each gas case. Except for the pure helium case, the arc temperature was found to be insufficient to produce any significant helium contribution to the spectra. Arc-temperature measurements indicated that the maximum temperature was on the order of 15,000 K. Measuring the hydrogen continuum radiation in the 562-nm region proved to be a convenient method for temperature determination, and calculation of arc temperature by use of a computer code indicated that knowledge of flow turbulence is extremely important as an input.

Comparison of computed and measured spectra over the wavelength interval investigated indicated that the RAD/EQUIL radiation code generally predicted the measurements except in the region near the Balmer limit where the predicted intensity was much less than the measured values. The radiation code was further used to show that the spectral distribution of radiation from the end of an arc heater would be different from a typical planetary entry shock layer at the same thermodynamic conditions because of the radial temperature distribution in the arc and the much greater plasma thickness of the arc relative to a shock layer.

Attempts to produce ablation gases from solid phenolic-carbon placed within the arc chamber were unsuccessful. Although the phenolic was quickly pyrolized from the material, the water-cooled walls conducted away sufficient heat to prevent significant ablation.

INTRODUCTION

The large gravitational potential involved in outer planet entry translates to potentially disastrous levels of radiative and convective heat flux which must be shielded from the spacecraft. Heat-shield designs involve direct payload tradeoffs and are based primarily on computer-model radiating flow-field calculations. These models rely on inputs and assumptions of which some aspects are often uncertain and experimentally unverified. Incomplete data deal with such fundamental variables as the composition of the planetary atmosphere as well as the presence and concentrations of ablation gases, some of which are purported to significantly reduce radiative heating loads. Differences in atmospheric composition affect the specific heat. The lower specific heat of helium-rich mixtures, for example, translates the braking kinetic energy of an entry probe into higher temperature of the shocked gases, with consequent higher radiation output. Information relating to ablation gases is even more significant since calculations indicate that they act as selective broadband filters shielding the spacecraft from the radiating plasma.

In reference 1, Moss et al. computed radiation absorption by ablation gases for a Jupiter entry where the heat shield was made of carbon-phenolic. The carbon molecules C_2 and C_3 were assumed to be the primary absorbers. Other hydrocarbons, for example C_2H, C_3H, and C_4H, were listed but not included in the calculations due to lack of thermodynamic and radiation absorption properties. In fact, property data for C_3 are quite limited. The only C_3 absorption data available from experiments were those of reference 2, until very recently when those data were extended by the shock tube work of reference 3 and the furnace experiment of reference 4.

The extreme heating rates of outer planet entry preclude exact simulation. In this investigation an arc heater was used to produce radiating hydrogen-helium plasma at 10^5 Pa (1 atm). H_2/He mass ratios were varied over the complete range while absolute axial spectral intensities were recorded from 130 to 850 nm. Spectroscopic temperature measurements, along with additional engineering data, were used to characterize the source. This information, in turn, was used to compute spectra with which to compare the axial measurements.

Attempts to introduce ablation products into the plasma are briefly described. The concept was to measure radiative flux with and without "blockage" to assess the model predictions.

SYMBOLS

I_ν	spectral intensity, W/cm^2-sr-nm
I_ν^i	incident spectral intensity, W/cm^2-sr-nm
j_ν	spectral emission coefficient, W/cm^3-sr-cm
k_ν	extinction coefficient, cm^{-1}
N	particle number density, cm^{-3}
p	pressure, Pa (10^5 Pa = 1 atm)
q	heat flux, W/cm^2
r	radius, cm
R	arc channel wall radius, cm
T	temperature, K
x	thickness, cm
τ_ν	optical depth, dimensionless
λ	wavelength, nm
θ	view angle

APPARATUS

An existing arc-heated materials-testing facility was modified and used as the basic equipment. The original facility consisted of the usual components of a high-temperature blowdown-type tunnel. Modification included removal of the nozzle, addition of all optical equipment, and replacement of the vacuum storage spheres by nitrogen operated ejectors.

The arrangement of the experimental equipment is shown in figure 1. Three major components made up the system: the arc heater, the spectral radiation-measurement monochromator with its optical system, and the plasma-temperature spectrometer with optics.

The plasma-temperature measuring system consisted of a spectrometer, a single-apertured lens, and a front-surface mirror. The mirror and lens were used to image a side view of the arc channel on the entrance slit of a 1-m modified Czerny-Turner spectrometer. The spectrometer and optics were mounted on a common movable platform which allowed movement of the total system for viewing the arc channel at different axial locations. The plasma was viewed normal to the heater axis through narrow (2-mm wide) quartz windows that had a height equal to the arc channel diameter.

The arc heater was a 2.4-cm inside-diameter, wall-stabilized unit which was constructed of alternate wafers of insulators and water-cooled, copper segments. Six of the copper segments were instrumented to obtain measurements of pressure, voltage, and wall heat flux. Three segments had windows for temperature measurement. A conical section formed the downstream 14 cm of the flow channel which increased to about 12-cm diameter at the exit. The test gas was heated by the arc which was struck from a hollow tungsten cathode at the upstream end to 32 water-cooled, copper-anode pins in the wall of the downstream conical section. A flat-faced cylindrical blunt body was located very near the exit and coaxial to the arc heater such that the heated gas was forced to turn and flow radially outward through a narrow gap into an evacuated chamber. The gap width was adjusted to provide the minimum flow area near the outer edge of the blunt body in order to assure subsonic flow within the flow channel which served as the source for the axial spectral measurements. A 0.76-mm diameter aperture located in the center of the blunt body face allowed radiation from the plasma to enter an optical tube leading to a 1-m vacuum ultraviolet scanning monochromator. The optical tube housed a concave platinum-coated mirror which focused the incident beam onto the monochromator entrance slit. A second aperture located in front of the mirror limited the view to an angle of 1.16° along the arc-channel centerline, and also determined the image size on the monochromator entrance slit. An S-20-type photomultiplier tube was used to detect the beam at the exit slit. A window that was coated with sodium-salicylate-phosphor was placed in front of the detector to facilitate measurement of the ultraviolet spectra. The entire optical system could be kept evacuated to a very low pressure, about 10^{-6} torr, since a calcium-fluoride-crystal window sealed the entrance end of the optical tube. A ball valve, located between the entrance aperture and the crystal window, isolated the optical system until the arc heater had reached a stable operating condition. Filters were mounted inside the optics tube and could be remotely inserted into the light path as needed for order-sorting. The equipment is described in more detail in reference 5. After initial tests, some modifications to the radiation-measuring optical system were required and are as follows:

(1) Mirror rotation controls were added and light sensors were located on each side of the monochromator entrance slit in order to maintain the incident beam on the slit during a test. This was necessary because stresses due to differential heating and pressure created small movements that were amplified by the optical lever arms. (2) Light sensors were also installed at points around the periphery of the mirror aperture to assure light-filled optics during both calibration and test. (3) A motor was used to provide remote-controlled movement of the blunt body to adjust the flow gap width after arc-heater ignition.

Optical Systems Calibrations

Temperature system.- The film on which the plasma intensity was recorded was calibrated by use of a tungsten secondary standard at the facility using a substitution scheme. The mirror which projected the arc image onto the spectrometer entrance slit was mounted in a holder which could be pivoted 90°. By pivoting the mirror the tungsten lamp image, instead of the plasma image, was projected onto the entrance slit. A laboratory sensitometer was used for relative calibration of the film.

Radiation spectra system.- The optical system used to measure the hydrogen-helium radiation was calibrated in place by a substitution technique. The arc heater was replaced by a lamp in which the source was the subliming anode of a carbon arc (see ref. 6). A fused silica lens was used to project a one-to-one image of the source onto the entrance aperture of the optical system. Corrections were made for the spectral transmission of the lens. This method was used for wavelengths greater than 280 nm. For shorter wavelengths, the sodium-salicylate-phosphor window was used to convert ultraviolet radiation to a wavelength of about 410 nm which could be sensed by the photodetector. Measurements of individual optical component transmission or reflectance and the quantum efficiency of the phosphor were used to determine the calibration relationship in this lower wavelength region. This method is described in detail in reference 5.

Operating Conditions

Because of electrical insulation constraints and the design power limit of the arc heater (1 MW), the maximum supply voltage utilized was 2000 V. The arc voltage drop (between cathode and anode) in hydrogen exceeds the voltage drop in helium by a factor of approximately 2.7 (see fig. 2). For any particular gas the voltage gradient is a function of pressure, and for this arc heater with a 2000-V supply, about 10^5 Pa (1-atm) pressure resulted in the maximum arc voltage allowable for a stable arc (about 1300 V for the pure hydrogen case). The remaining voltage drop is required across ballast resistance in the circuit. In order to stay within the 1-MW design power limit of the arc heater then, the arc current could not exceed 800 amperes. Consequently, a constant arc operating condition of 800 A at 10^5 Pa (1-atm) pressure was selected for all gas compositions. Available increments in power supply voltage were 1000 V. Arc impedance in pure helium and 80-percent helium allowed use of the 1000-V setting.

4

RESULTS AND DISCUSSION

Hydrogen and helium, elements with the simplest atomic structure, have been extensively studied and their individual atomic spectra are well known. The emission spectra are modified significantly by the gas environment, but many of the environmental effects can be theoretically predicted, provided all of the thermodynamic and radiative conditions are known. However, in a working arc facility with sharp gradients and electric fields, it is not obvious that the pertinent conditions are well defined, especially for gas mixtures. On the other hand, spectroscopic measurements in the harsh environment of an arc-heater exhaust are not a trivial undertaking, and furthermore, it may be desirable to predict the spectra from an arc heater of different size and operating conditions. The emission intensity equation can be solved quickly with high-speed computers if local thermodynamic equilibrium is assumed and sufficient information is provided to determine the spectral absorption coefficient, k_ν. In reality, the equations relating k_ν to number density and temperature become quite complicated (e.g. see ref. 7) and invariably, assumptions and approximations are necessary to make the relations more tractable.

The radiation computer code RAD/EQUIL (ref. 8) was used to compute the spectral radiant intensity for comparison to the measured data. For inputs, the code requires the gas composition, temperature, and pressure at a sufficient number of points to describe the radiation path.

The temperature and pressure were measured at several points along the arc for input to the radiation code. In general, however, it would be better to be able to accurately predict these parameters for any size arc heater or operating conditions. The arc-heater code (ARCFLO) was used to compute the arc parameters. The ARCFLO program is based on the work of Watson and Pegot (ref. 9) and modified versions were reported in references 10 and 11. Other modifications have been made since these publications.

The arc parameters (temperature, pressure, gas composition) and spectra from the axial view are discussed in the two following sections. A third section relates some of the experience with solid ablator efforts.

Arc Parameters

Temperatures and gas composition.- Photons escaping from a source can carry information about its interior. Using conservation of energy, it is easy to show that the transfer is governed by the equation:

$$\frac{d\, I_\nu}{d\,\tau_\nu} = j_\nu / k_\nu - I_\nu \tag{1}$$

where I_ν is the spectral intensity [radiant power/(projected area · solid angle · frequency interval)], j_ν is the emission coefficient [radiant power/(volume · solid angle · frequency interval)], k_ν is the extinction coefficient [length^{-1}] which reduces to the linear absorption coefficient in the absence of scattering, and the optical depth τ_ν is its line integral viz.,

$$\tau_\nu = \int k_\nu \, dx \tag{2}$$

Most diagnostic applications rely on the slab solution which, with incident radiance I_ν^i, is

$$I_\nu = j_\nu/k_\nu \, (1-e^{-\tau_\nu}) + I_\nu^i \, e^{-\tau_\nu} \tag{3}$$

In the "optically thick" limit as $\tau_\nu \to \infty$ the measurement determines j_ν/k_ν directly. This ratio, known as the source function, is identifiable with the Planck black-body radiance for most laboratory-based observations. Under such conditions the spectral detail is irrelevant and standard pyrometry can be used to assess the temperature. This condition is approached when viewing along the arc axis in the spectral regions of strong lines such as H_α, but observations are hampered by the unknown properties of the rapidly declining temperature layer which separates the arc column from the entrance aperture of the optical system.

The opposite limit is of wider applicability. "Optical thinness" is said to prevail when the exponential of equation 3 is adequately represented by its linear approximation. Then (for $I_\nu^i = 0$)

$$I_\nu = \int j_\nu \, dx \tag{4}$$

that is, the measured radiance is the spatial integral of the emission coefficient which can trivially be recovered for homogeneous conditions. In the most interesting case of cylindrical symmetry, a simple change from rectangular to cylindrical coordinates results in

$$I_\nu(x) = 2 \int_{r=x}^{r=R} \frac{j_\nu(r) \, r \, dr}{(r^2-x^2)^{1/2}} \tag{5}$$

which can be (Abel)* inverted to give

---

*For a complete discussion of the Abel inversion technique as applied to cylindrical arcs, see reference 12.

$$j_\nu(r) = \frac{1}{2\pi r} \frac{d}{dr} \left[2 \int\limits_{r=x}^{r=R} \frac{I_\nu(x)}{(x^2-r^2)^{1/2}} \, x \, dx \right] \qquad (6)$$

Use of the diagnostic "side-view" system allowed the determination of absolute emission coefficients. Photographic recording simplifies the facility application.

To describe the plasma-temperature field for this study, a spectrometer was used to record on film the total continuum emission intensity from all hydrogen constituents centered at a wavelength of 562 nm. The plasma compositions were calculated with the ACE computer program described in reference 13, and figure 3 shows the number densities for the different species of a pure hydrogen plasma at a total pressure of 10^5 Pa. This method (use of the total continuum emission) which is a proposed calibration standard (ref. 14) sidesteps some of the problems associated with use of single-component continuum emission or line radiation. For example, it is generally true that a particular constituent like H, e^-, H^-, etc. increases with temperature and then diminishes or levels off. This can make for insensitive temperature measurement or even double valuedness. In line-radiation methods, complications involve discrimination of one spectral feature in the presence of competing processes. Some hydrogen lines, for instance, broaden to the extent that they merge and line-shape corrections must be introduced to compensate, thus degrading accuracy. The chosen spectral region for this study was the total continuum in the 500- to 600-nm range which is essentially devoid of line radiation. The emission coefficient has molecular, atomic, and ionic contributions which contribute additively to help defer the temperature insensitivity limit to 15,000 K or 16,000 K. The intensity calculation is reliable to 2 percent over the range of interest. To infer temperature, measured and calculated j_ν values must be compared. Roberts and Voigt (ref. 15) tabulate the spectrum from 8,000 K to 16,000 K over the wavelength range of 400 nm to 15,000 nm, listing also the fractional contributions. Representative values are shown in figure 4 for pure hydrogen at 13,000 K along with RAD/EQUIL (ref. 8) output for the same conditions.

To extend the range of the Roberts and Voigt (ref. 15) data and to accommodate the admixture of He, their equation (1) was programed. Values for $F(\lambda,T)$, the emission coefficient for H_2^+ per neutral hydrogen atom and proton; $G(\lambda,T)$, the emission coefficient for H^- per neutral hydrogen atom and electron as well as free-free and free-bound Gaunt factors were Lagrange interpolated from tables in the Roberts and Voigt paper and supplemented using extensive values from Drawin and Felenbok (ref. 16). The pertinent calibration coefficients are shown in figure 5 along with the discrete values provided in the published reference. Since helium lines are narrow and easily identifiable, they do not interfere with the efficacy of using the hydrogenic continuum when mixtures are run.

Typical results of the temperature measurements are shown in figure 6 along with computed values from ARCFLO. These radial distributions are for the pure hydrogen case and were taken at three different axial locations along the arc

column as indicated on the accompanying sketch. It is obvious that the computed values are highly sensitive to assumptions about flow turbulence. The computed laminar-flow temperature at the centerline is about 26,000 K whereas the turbulent-flow value is about 15,000 K. The measured centerline values are in better agreement with the turbulent predictions but the measured profiles are flatter than the computed values. From these data, turbulent flow may appear to be a reasonable assumption, however, comparison of all parameters (e.g. arc voltage, wall heat flux) for all gas-mix cases did not substantiate this. Previous experience with arc-heater computer codes indicate that predictions can be brought into better agreement with experiment when the code is tailored to the particular arc heater and general operating conditions of interest. Since the computed spectrum is quite temperature sensitive, a temperature versus axial distance curve was constructed for each hydrogen-bearing case (the pure helium temperature was not measured) based on the measured centerline temperatures. These curves were used for temperature input to the radiation program. Actually the "end-view" optical system has a field of view which includes gas temperatures different from the centerline values. Although the view angle is small (1.16°) almost one-half the radius falls within view at the upstream end of the arc channel. Figure 7 presents the axial distributions of temperature at the centerline and off-axis for the pure hydrogen case. The effect of the off-axis temperature variation on measured spectra is discussed in a following section.

The maximum measured temperature of about 15,000 K which occurred at the arc centerline remained approximately the same regardless of the gas mixture (helium temperature not measured).

Pressure.- The pressure was measured through small orifices located at six points along the arc channel. A typical axial pressure distribution is shown in figure 8 which includes both measured and computed values. The assumption of laminar or turbulent flow is seen to have little effect on the computed pressure. The pressure is assumed to be constant in the radial plane for both computed and measured values.

Spectra.- As previously mentioned, the spectrum from the end-view was both computed and measured for each gas except the pure helium case. The computer program did not contain radiative properties for helium although it did contain helium thermodynamic and transport properties. The lower wavelength limit was determined by the optical cutoff of the calcium fluoride window in the measurement system. Similarly, the upper bound was determined by the decrease in sensitivity of the optical system. Within this spectral region a comparison of spectra for a 1-cm length of pure hydrogen plasma at 13,000 K is shown in figure 4 for the computer program (RAD/EQUIL) and the tabulated values of Roberts and Voigt (ref. 15). (Compare the total line + continuum values). Roberts and Voigt do not include values for the group of lines in the spectral region from about 360 nm to 530 nm.

The measured spectra for the four different gas cases are shown in figure 9. Figure 9(a) shows the pure helium spectrum which consists mostly of very narrow lines and an appreciable amount of continuum in the ultraviolet region. All of the lines were identified and found to be due to He I. The pure hydrogen spectrum in figure 9(b) exhibits the Stark broadened lines of the Balmer series and the ultraviolet continuum which accounts for most of the radiation. The spectra for the two mixture cases in figure 9(c) and figure 9(d) show that the radiation is due to hydrogen. The only evidence of helium is the very small contribution

of the line at 587.6 nm which is seen to be the most intense of the helium spectrum in figure 9(c). The helium simply served to reduce the number of hydrogen radiators and thereby reduced the total radiation. Since the centerline temperature remained in the neighborhood of 15,000 K for all hydrogen-bearing cases, the helium was not hot enough to emit significant radiation. Consequently, for fixed arc current, the pure hydrogen produced a representative spectrum with the greatest magnitude and for the least complexity in diagnostics and operation.

Representative of the computed spectra is the pure hydrogen spectrum shown in figure 10 along with the measured spectrum. For most wavelengths the computed magnitude is greater and the lines are broader than the measured values. These features are indicative of a higher temperature. Recall that the gas in the arc channel exhibited a radial temperature distribution and that the axial centerline values were used as program inputs. The lower values and more narrow lines in the measured data probably result from the fact that the small view angle of the optical system encompasses more of the temperature field than just the centerline values. This effect was demonstrated by using the two extreme measured temperature distributions shown in figure 7 where one distribution is along the arc centerline and the other is along the edge of the view angle. These results, shown in figure 11, serve as a reminder that the measured spectrum will reflect the effect of temperature for all of the gas within the field of view.

Referring again to figure 10, another obvious difference is the apparent continuum in the region of the Balmer limit (near 380 nm) that appears in the measured spectrum but not in the computed one. This continuum results from the merger of many broadened lines (apparent continuum) as the series limit is approached and also due to the lowering of the hydrogen ionization potential (real continuum) by the plasma microelectric field (see refs. 15 and 17). All of the line radiation from the Balmer limit through the Balmer γ (H_γ) line is included in a line "group" in the computer program and is represented by the H_δ and H_γ lines in the computed spectrum. Although the area under these two lines is greater than the measured value, it does not appear to be sufficient to account for the missing continuum in this region. This wavelength increment is not large, but it is important for planetary entry considerations since absorption by the heat-shield ablation product C_3 is reported to be at a maximum in this region.

As mentioned earlier, simulation of the spectral distribution of outer planet entry radiation is desirable because of the spectral absorption characteristics of ablation gases. The following discussion points out the difficulty in achieving this simulation however, due to the nature of the arc itself. In order to accommodate an acceptable size of materials sample, an arc heater suitable for planetary-entry simulation would require much larger physical dimensions, and consequently, greater power input than the heater reported here. Such a heater, reported in reference 18, has a length of about 5 m, an inside diameter of 6 cm, and operates at about 5,000 amperes and 6×10^5 Pa (6-atm) pressure. This arc current and diameter provides about the same average current density obtained in the heater reported here operating at 800 amperes. Consequently, the arc temperature would be expected to have approximately the same value. Computations with the arc-heater code using a turbulent-flow assumption revealed a centerline temperature distribution within the range of 16,000 K to 14,000 K and pressure distribution between 6 and 5 atm. Using these values and the 5-m length for

input to the radiation code for a 50/50 hydrogen-helium mixture by mass, the spectrum was computed and is presented in figure 12. For this case, it is evident that the lines are unimportant and the continuum approaches a black-body limit with the ultraviolet region being the most important. A 15,000 K black-body curve is shown for reference. From equation (3), it is evident that the intensity will approach the black-body value as the path length x becomes very large $(\tau_\nu \sim k_\nu x)$. The shock thickness, however, even for the Jupiter entry case (ref. 1) is on the order of centimeters. Using the same temperature and pressure distributions, x was changed to 3 cm and these computed results were plotted on the same figure. Obviously the shock-produced spectrum where line radiation is important is quite different from the arc-produced spectrum. In an entry simulation facility where a materials sample is immersed in the supersonic exhaust, the intensity incident on the sample would be the resultant of the arc and shock radiation, subject to any interaction within the shock layer. Consequently, the arc radiation must be taken into consideration when simulation of planetary entry radiation spectral distribution is desirable. Of course, the actual temperature and pressure behind the shock would depend on the flow Mach number and sample shape according to conventional shock relations. Finally, this study has been of emission from the hottest core region of the arc and off-axis emission would be expected to be less due to the decrease in radial temperature. However, when the temperature decreases sufficiently across the arc-channel radius to allow molecular species, molecular hydrogen becomes a strong radiator in the vacuum ultraviolet (ref. 15). In a study of a very small hydrogen arc heater proposed as a standard vacuum ultraviolet light source, Ott et al. (ref. 19) reported an off-axis radiation at a wavelength of 160.6 nm that was on the order of 100 times the centerline value. The off-axis emission was attributed to the Lyman bands of molecular hydrogen. The arc centerline temperature was reported to be 19,500 K and at a pressure of 1 atm.

Solid ablator efforts.- Two attempts were made to observe ablation product absorption of the hydrogen radiation due to ablation of solid material in the combined convective-radiative heating environment. One test involved material mounted at the blunt-body face and in the second case the material was mounted on the arc channel side wall. In both cases observations were made in the 400-nm wavelength region where the triatomic carbon molecule (C_3) is a strong absorber. No absorption was observed in either case. The two cases are briefly discussed in the following paragraphs.

In the first case the material sample was mounted in the center of the flat face of the blunt body and contained the entrance aperture to the "axial-view" optical system. The original blunt body configuration included a 2.54-cm diameter cylindrical plug centered in the flat face of the blunt body. This plug was separately cooled and contained the optical system entrance aperture as well as numerous small holes for injection of simulated ablation gases. (Some results of injected-gas absorption are reported in ref. 20). This original plug was replaced by one made of phenolic carbon (see the sketch in fig. 13). A small amount of pure cold helium was bled outward through the surface in order to prevent the flow of hot gas into the optical system and subsequent damage to the calcium-flouride-crystal window. The plug side walls were sealed with the main blunt-body interior wall which resulted in conductive cooling of the plug. The plug face wall was about 0.635-cm thick and when exposed to the plasma charred to a depth of about 2 to 3 mm but, in general, the char remained intact. Surface temperature, determined by a photographic pyrometer sighted through a specially machined port, was approximately 2,300 K, insufficient for graphite sublimation. Localized surface erosion to a depth of several millimeters randomly occurred in location and time, possibly due to temporary arc attachment.

The second case involved carbon-phenolic rings which were cut to fit concentric with the inside surface of the arc channel. As shown in the sketch of figure 14, the total length of ablator was 4 cm, although it was necessary to segment the material in order to avoid arc shunting at the wall. The entrance and exit to the ablator section were tapered and the central portion was a constant diameter of 1.524 cm. Other pertinent dimensions are given in the sketch. Each material segment was fitted to a corresponding water-cooled copper segment which made up the original arc channel. The copper segments were separated by boron nitride insulators and the carbon-phenolic rings were separated by an open gap. The boron nitride insulators are cooled by contact with the adjacent copper walls. Windows (normally used for arc-temperature measurement) were located 0.84-cm upstream and downstream of the material so that with a specially devised split optical system both regions could be spectroscopically observed at the same wavelength simultaneously. The "temperature" spectrometer was used for these observations. Comparison of spectra obtained from upstream and downstream of the material showed negligible differences. Removal and inspection of the material by sectioning after the test showed that the material was completely charred. Weight measurements indicated that the char density was nearly identical to that obtained in static furnace tests in reference 21. Dimensional changes in the material were imperceptible. Apparently the phenolic was pyrolized from the material almost immediately after arc ignition but heat conduction to the copper wall was sufficient to allow survival of the carbon char. Unfortunately the sequence of events necessary for arc ignition and adjustment to stable operating conditions required about 15 to 20 seconds. Three consecutive tests with an accumulation time of 245 seconds produced no appreciable change in the char. The axial distributions of pressure and heat transfer to the arc channel wall (determined by cooling water flow rate and temperature rise) are shown in figure 15 for flow with and without the material samples installed. Flow turbulence was apparently increased by the carbon inserts as evidenced by the jump in wall heat flux immediately downstream of the samples. The material samples were located about midway the constant diameter arc channel in order to reduce the probability of flow disturbances near the electrodes and also to provide a more favorable radiative flux. Earlier computer studies (ref. 22) showed that the radiative flux was greatest near the upstream end whereas convective heating was greatest near the downstream end. The measured heating rate in figure 15 is due to the combined convective and radiative flux. The predicted peak-radiative heating alone during Jovian entry would exceed the combined peak-arc-channel values shown here by a factor of about 35 (ref. 1). Although simulation of heating rates of this magnitude are unlikely, graphite could probably be ablated if insulation was provided between the graphite and the cold wall. Insulation which might result in spectroscopic contamination, however, would be undesirable. A pure graphite would be more desirable as an ablator than a phenolic-carbon composite since the phenolic is quickly volatilized. A further desirable feature would be an optical system with instant broad-band coverage since the steady-state ablation process would likely occur for only a matter of seconds due to the change in geometry.

CONCLUDING REMARKS

A study of hydrogen-helium plasma temperature and spectra in the wavelength interval 130 to 850 nm in a wall-stabilized arc heater leads to the following concluding remarks. Measurements were made with the arc heater operating at 800-A and 10^5 Pa (1-atm) pressure.

The maximum temperature measured, which was at the arc centerline, was on the order of 15,000 K for hydrogen and both mixtures tested. The hydrogen-plasma temperature can be conveniently determined by spectroscopic techniques using the hydrogen continuum radiation in the wavelength neighborhood of 562 nm.

A computer model overpredicted the arc centerline temperature by about 75 percent when laminar flow was assumed. When turbulent flow was assumed the predicted centerline temperature was within about 10 percent of the measured values at most axial locations, but the predicted radial distributions decreased more rapidly than did the measurements.

When hydrogen and helium are mixed, even as much as 80-percent helium by mass, the arc-radiation spectral distribution remains a hydrogen spectrum since the temperature is not high enough to produce significant helium radiation.

The arc-heater plasma radiation can be predicted within the accuracy of the measurements by radiation computer code RAD/EQUIL (ref. 8) over most of the spectra investigated. However, radiation intensity near the Balmer series limit is greatly underpredicted and although this deficiency occurs over a short wavelength span, it is an important region for planetary entry considerations because of the absorption by the ablation product C_3 which peaks near these wavelengths.

Since the plasma in the arc channel has a radial temperature distribution, measurement of spectra from a particular arc channel region requires a narrow-view angle in order to avoid averaging the recorded spectra which reflect the variation in source temperature.

When the arc plasma is at the same thermodynamic conditions as the shock layer created by a Jovian entry probe, the spectral distribution of the arc radiation will be approximated by a black-body distribution which is highly shifted to the ultraviolet relative to the shock radiation. This is simply due to the much greater length of the arc relative to the shock layer.

For the experimental conditions reported here, carbon-phenolic ablation material used in entry simulation tests will require insulation from the cooled facility components in order to produce significant carbon ablation. Tests showed that the phenolic quickly pyrolized from the material however, even without insulation from the wall.

12

REFERENCES

1. Moss, James N.; Jones, Jim J.; and Simmonds, Ann L.: Radiation Flux
    Penetration Through a Blown Shock Layer for Jupiter Entry Conditions.
    AIAA Paper 78-908, May 1978.

2. Brewer, Leo; and Engelke, John L.: Spectrum of C_3. J. Chem. Phys., vol. 3,
    no. 4, February 1962, pp. 992-998.

3. Jones, Jim J.: The Optical Absorption of Triatomic Carbon C_3 for the
    Wavelength Range 260 to 560 nm. NASA TP 1141, 1978.

4. Snow, Walter L.; and Wells, William L.: The Spectral Opacity of Triatomic
    Carbon Measured in a Graphite Tube Furnace Over the 280 to 600 nm
    Wavelength Range. To be published in J. Chem. Physics.

5. Wells, William L.; and Snow, Walter L.: Apparatus for Experimental Investi-
    gation of Aerodynamic Radiation With Absorption by Ablation Products.
    NASA TM X-3467, March 1977.

6. Hattenburg, Albert T.: Spectral Radiance of a Low Current Graphite Arc.
    Appl. Opt., vol. 6, no. 1, January 1967, pp. 95-100.

7. Lasher, L. E.; Wilson, K. H.; and Greif, R.: Radiation from an Isothermal
    Hydrogen Plasma at Temperatures Up to 40,000° K. J. Quant. Spect. and
    Radiat. Transfer, vol. 7, 1967, pp. 305-322.

8. Nicolet, W. E.: User's Manual for the Generalized Radiation Transfer Code
    (RAD/EQUIL). Rep. No. UM-69-9 (Contract NAS1-9399), Aerotherm Corp.,
    October 1969. (Available as NASA CR 116353).

9. Watson, V. R.; and Pegot, E. B.: Numerical Calculations for the Characteris-
    tics of a Gas Flowing Axially Through a Constricted Arc. NASA TN D-4042,
    June 1967.

10. Nicolet, W. E.; Shepard, C. E.; Clark, K. J.; Balakrishnan, A.;
    Kesselring, J. P; Suchsland, K. E.; and Reese, J. J.: Methods for the
    Analysis of High-Pressure, High-Enthalpy Constricted Arc Heater.
    AIAA Paper 75-704, May 1975.

11. Nicolet, W. E.; Shepard, C. E.; Clark, K. J.; Balakrishnan, A.;
    Kesselring, J. P.; Suchsland, K. E.; and Reese, J. J.: Analytical and
    Design Study for a High-Pressure, High-Enthalpy Constricted Arc Heater.
    Report No. 74-125, prepared for AEDC, AF Contract No. F40600-74-C-0015,
    Aerotherm Division, Acurex Corporation, Mountain View, California,
    November 1974.

12. Snow, Walter L.: Practical Considerations for Abel Inverting of Photographic
    Data With Application to the Analysis of a 15-kW Wall-Stabilized Arc-Light
    Source. NASA TN D-6672, 1972.

13. Powars, Charles A.; and Kendall, Robert M.: User's Manual--Aerotherm
    Chemical Equilibrium (ACE) Computer Program. Aerotherm Corp., May 1969.

14. Behringer, K.; and Thomas, P.: VUV Radiometry Below 100 nm: The High-Power Hydrogen Arc as a Standard Source of Continuum Radiation Between 53 nm and 92 nm. Applied Optics, vol. 18, no. 15, August 1979, pp. 2486-2594.

15. Roberts, J. R.; and Voigt, P. A.: The Calculated Continuous Emission of a LTE Hydrogen Plasma. J. of Research of the NBS-A, Physics and Chemistry, vol. 75A, no. 4, July-August 1971, pp. 291-298.

16. Drawin, H. W.; and Felenbok, P.: Data for Plasmas in Local Thermodynamic Equilibrium. Gauthier-Villars, Paris, 1965.

17. Nelson, H. F.; and Goulard, R.: Equilibrium Radiation from Isothermal Hydrogen-Helium Plasmas. J. Quant. Spect. and Radiat. Transfer, vol. 8, 1968, pp. 1351-1372.

18. Davey, W. C.; Menees, G. P.; Lundell, J. H.; and Dickey, R. R.: Carbonaceous Materials Subject to Extreme Heating: A Comparison of Numerical Simulation and Experiment. AIAA/ASME Paper 78-866, May 1978.

19. Ott, W. R.; Behringer, K.; and Gieres, G.: Vacuum Ultraviolet Radiometry With Hydrogen Arcs. 2: The High-Power Arc as an Absolute Standard of Spectral Radiance From 124 nm to 360 nm. Applied Optics, vol. 14, no. 9, September 1975, pp. 2121-2128.

20. Walberg, G. D.; Wells, W. L.; Houghton, W. M.; and Midden, R. E.: PERF: A New Approach to the Experimental Study of Radiative Aerodynamic Heating and Radiative Blockage by Ablation Products. AIAA Paper 74-1272, October 1974.

21. Engelke, W. T.; Pyron, C. M., Jr.; and Pears, C. D.: Thermal and Mechanical Properties of a Nondegraded and Thermally Degraded Phenolic-Carbon Composite. NASA CR-896, 1967.

22. Wells, William L.: Experimental Investigation of a Wall-Stabilized Arc With Comparisons to Theoretical Predictions. M.S. Thesis, George Washington University, June 1973.
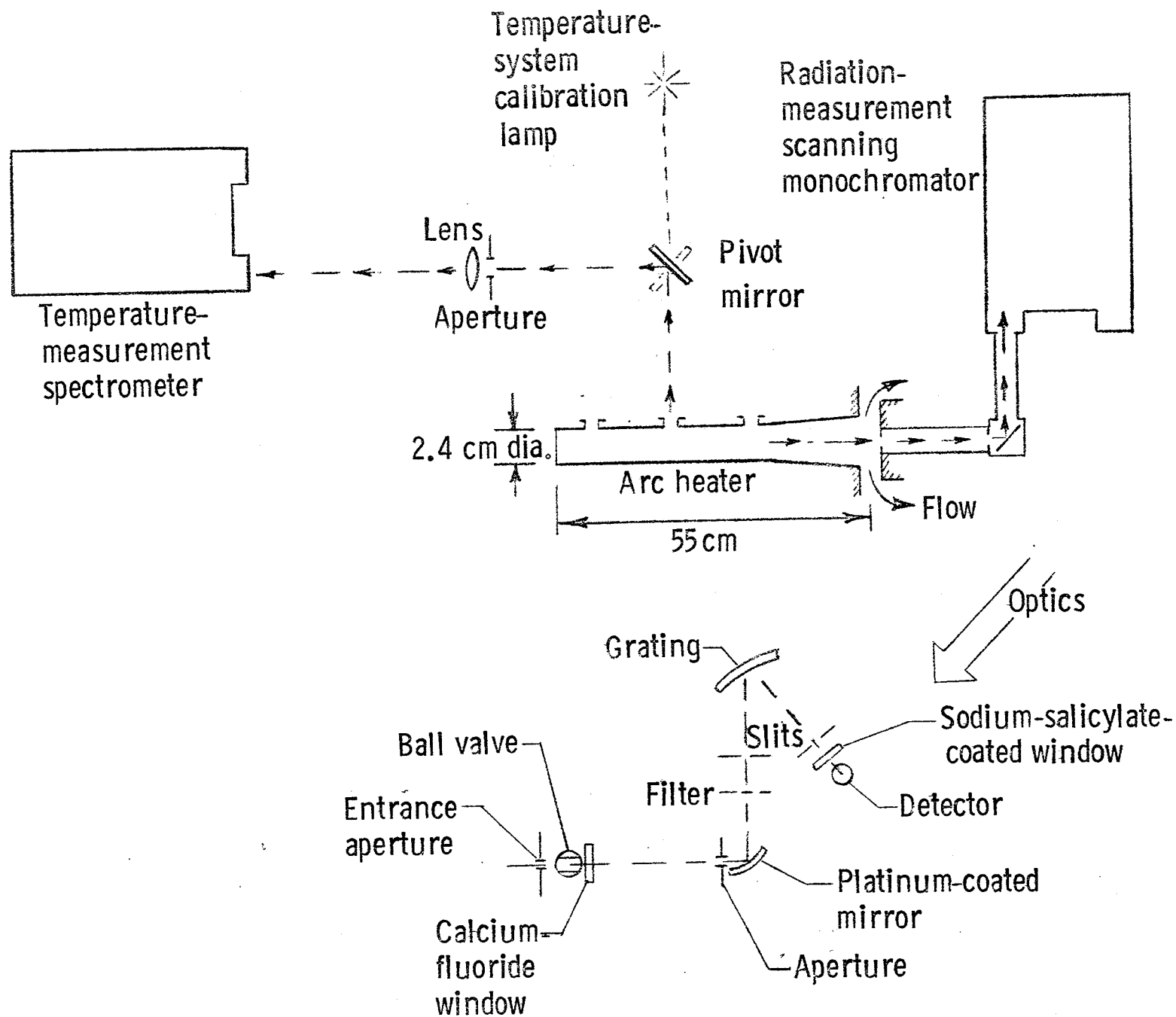
Figure 1.- Arrangement of experimental equipment.
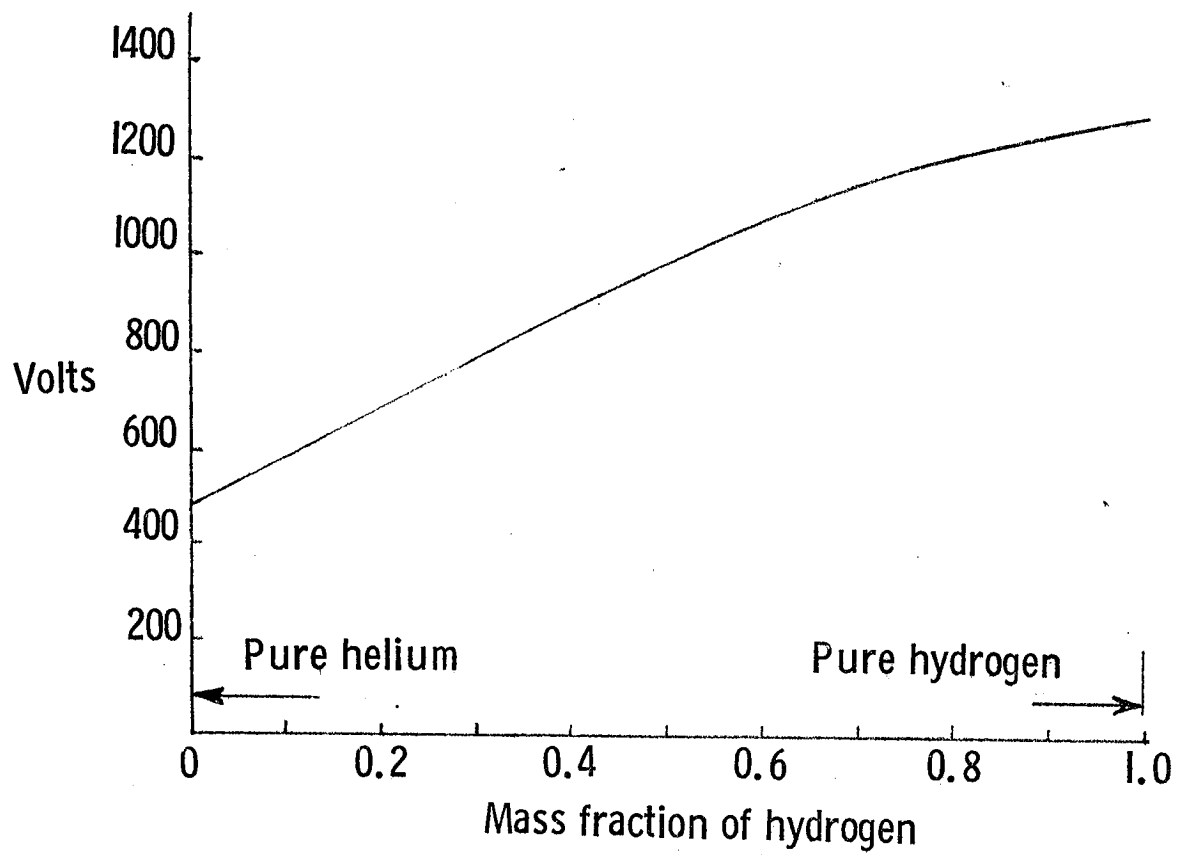
Figure 2.- Measured arc voltage in hydrogen-helium at 800 A and 10^5 Pa (1 atm).
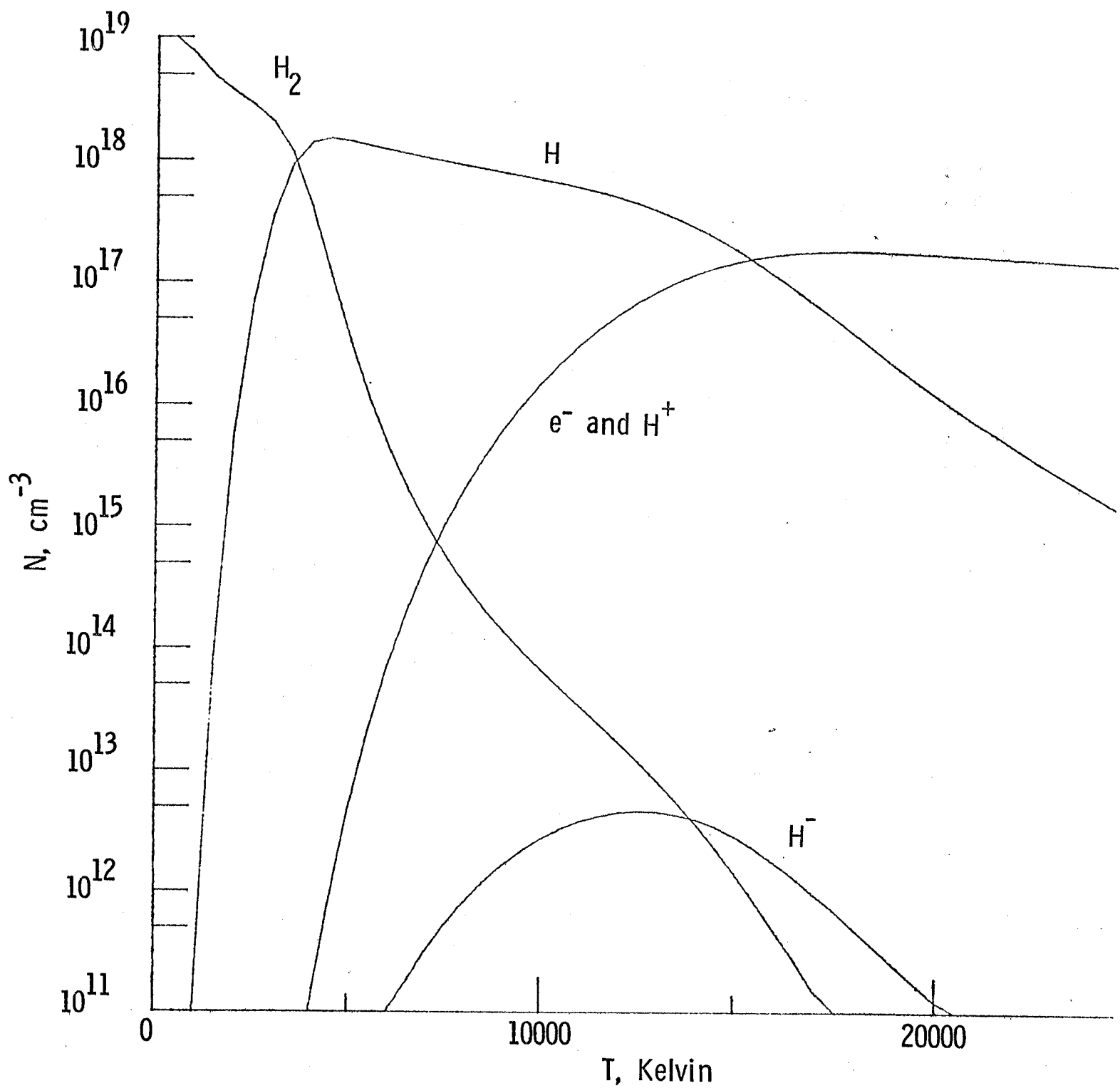
Figure 3.— Hydrogen-plasma composition computed with ACE program at 10^5 Pa (1 atm).
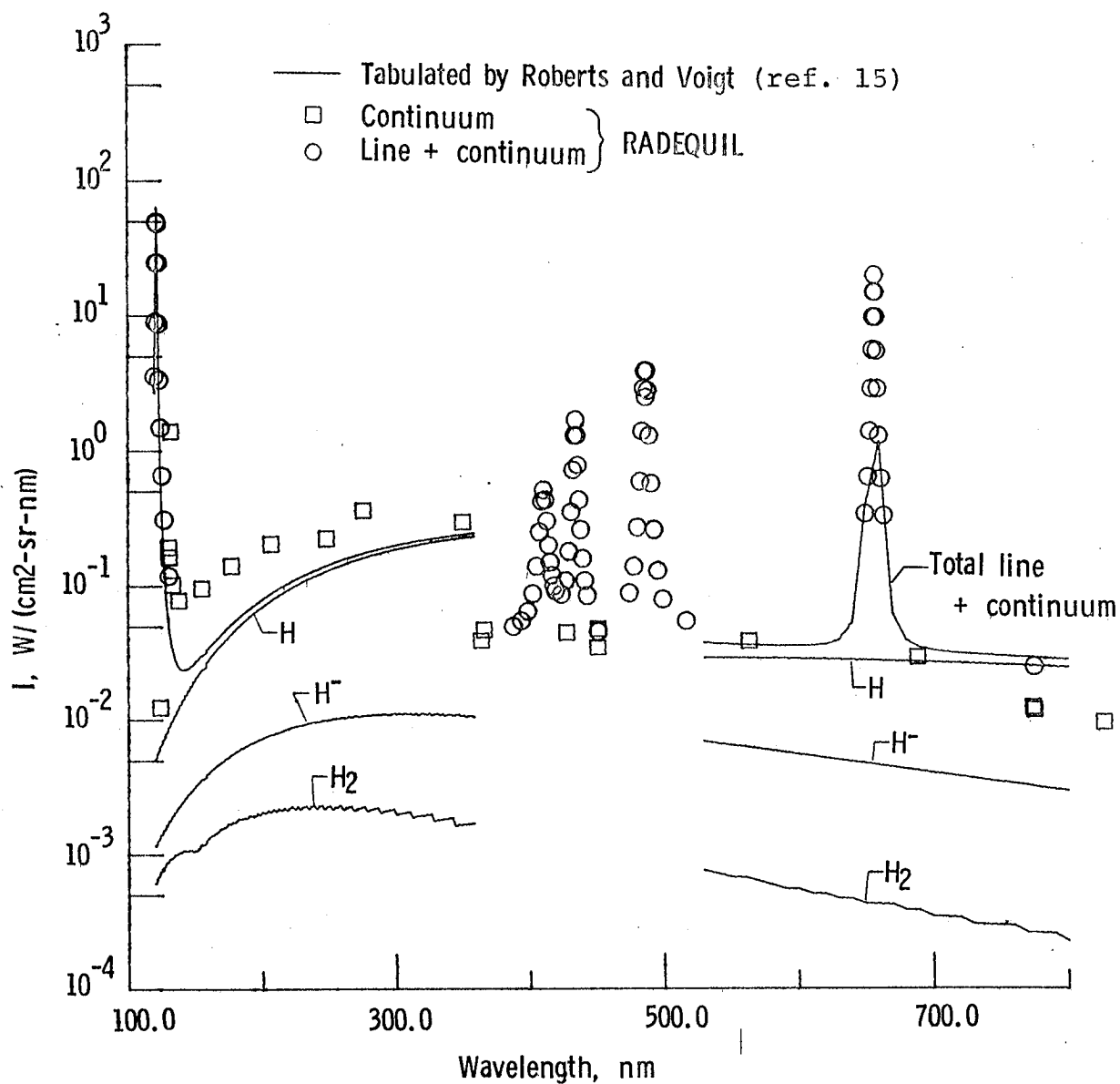
Figure 4.– Calculated spectrum for 1-cm thickness of hydrogen-plasma at 13,000 K and 10^5 Pa (1 atm) in the wavelength interval 110 to 800 nm.
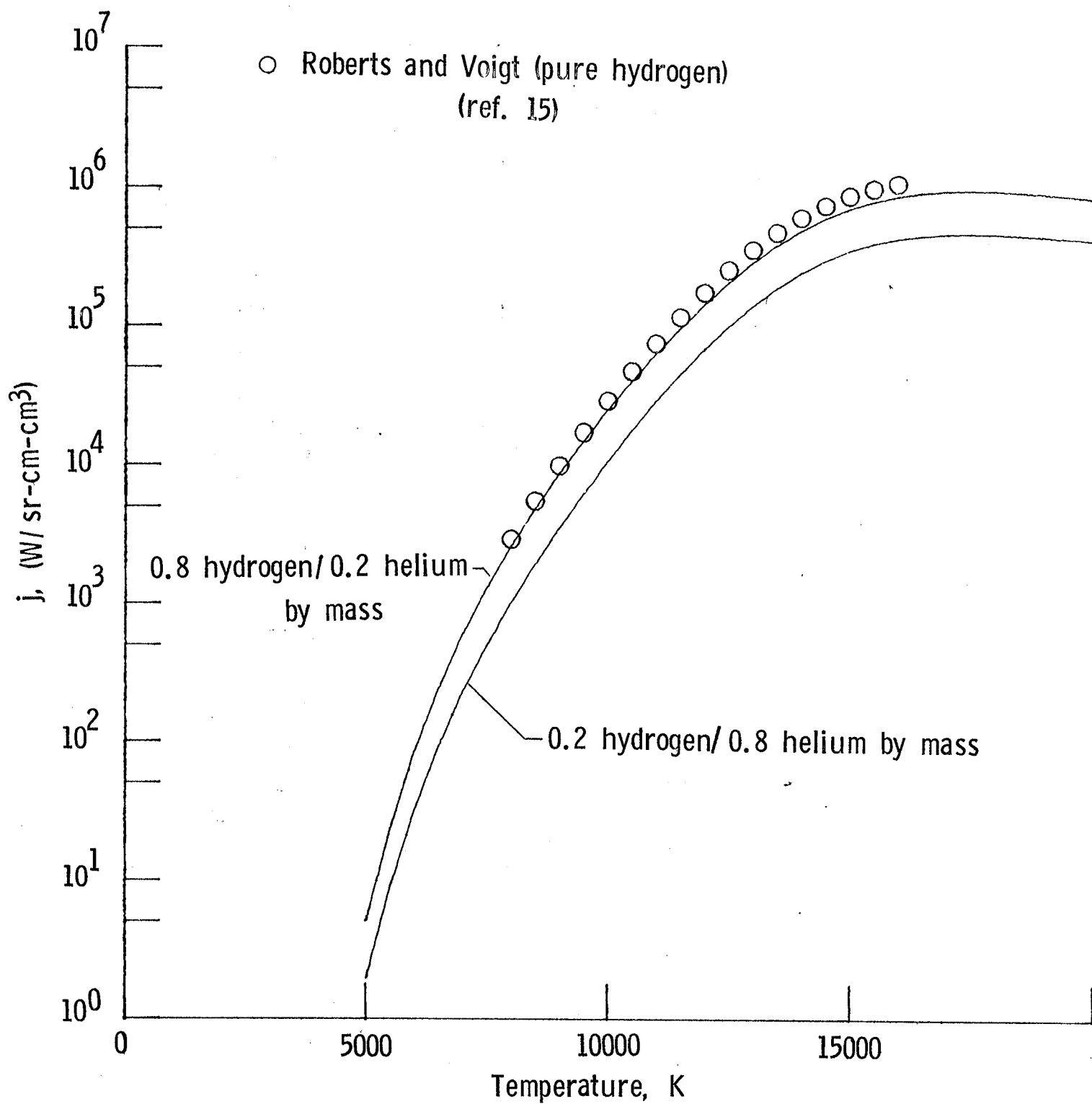
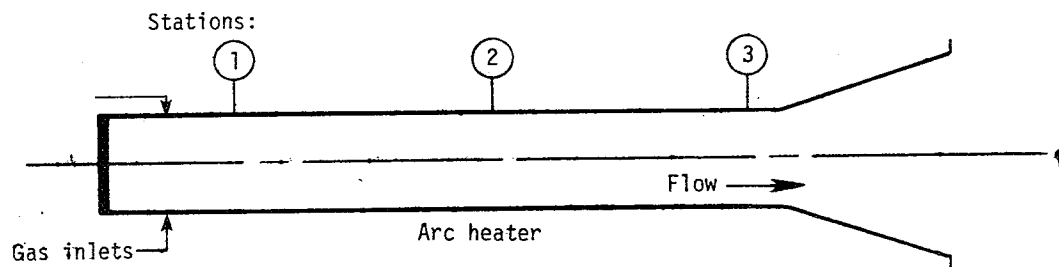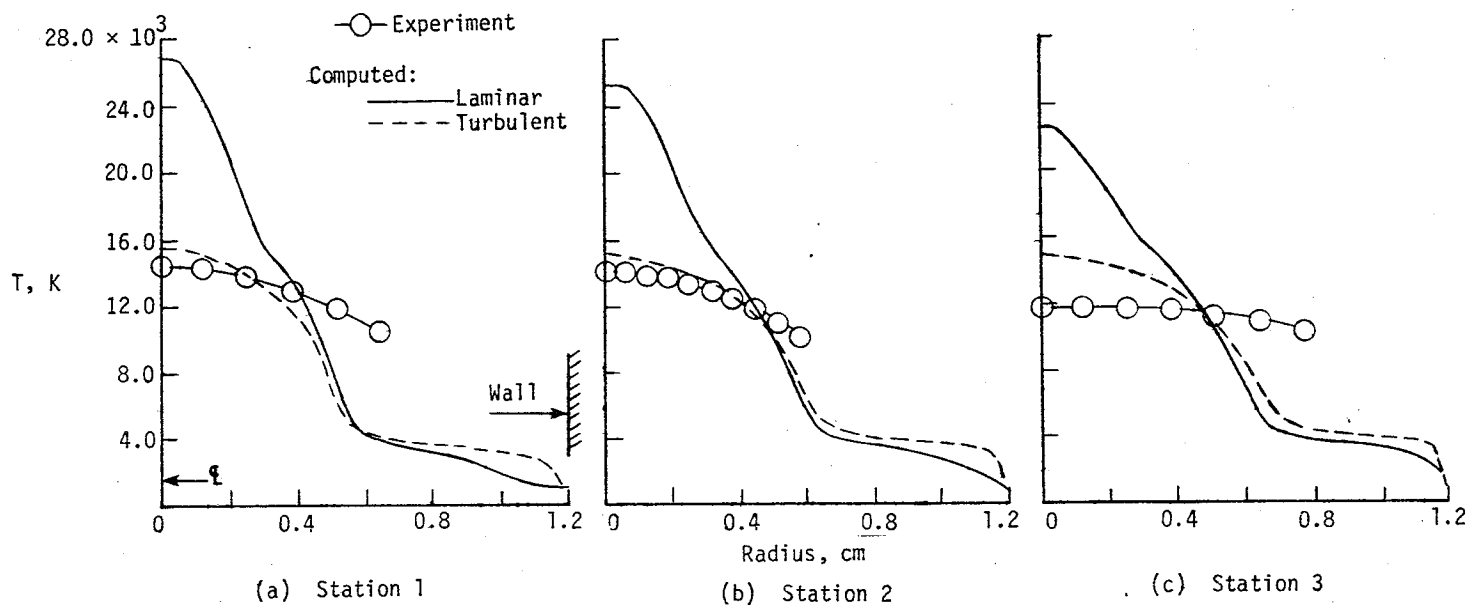Figure 5.– Hydrogen volume emission coefficient for total continuum at 550 nm for total pressure of 10^5 Pa (1 atm).

Figure 6.- Measured and computed radial-temperature distributions at three axial locations in the arc heater operating with pure hydrogen.
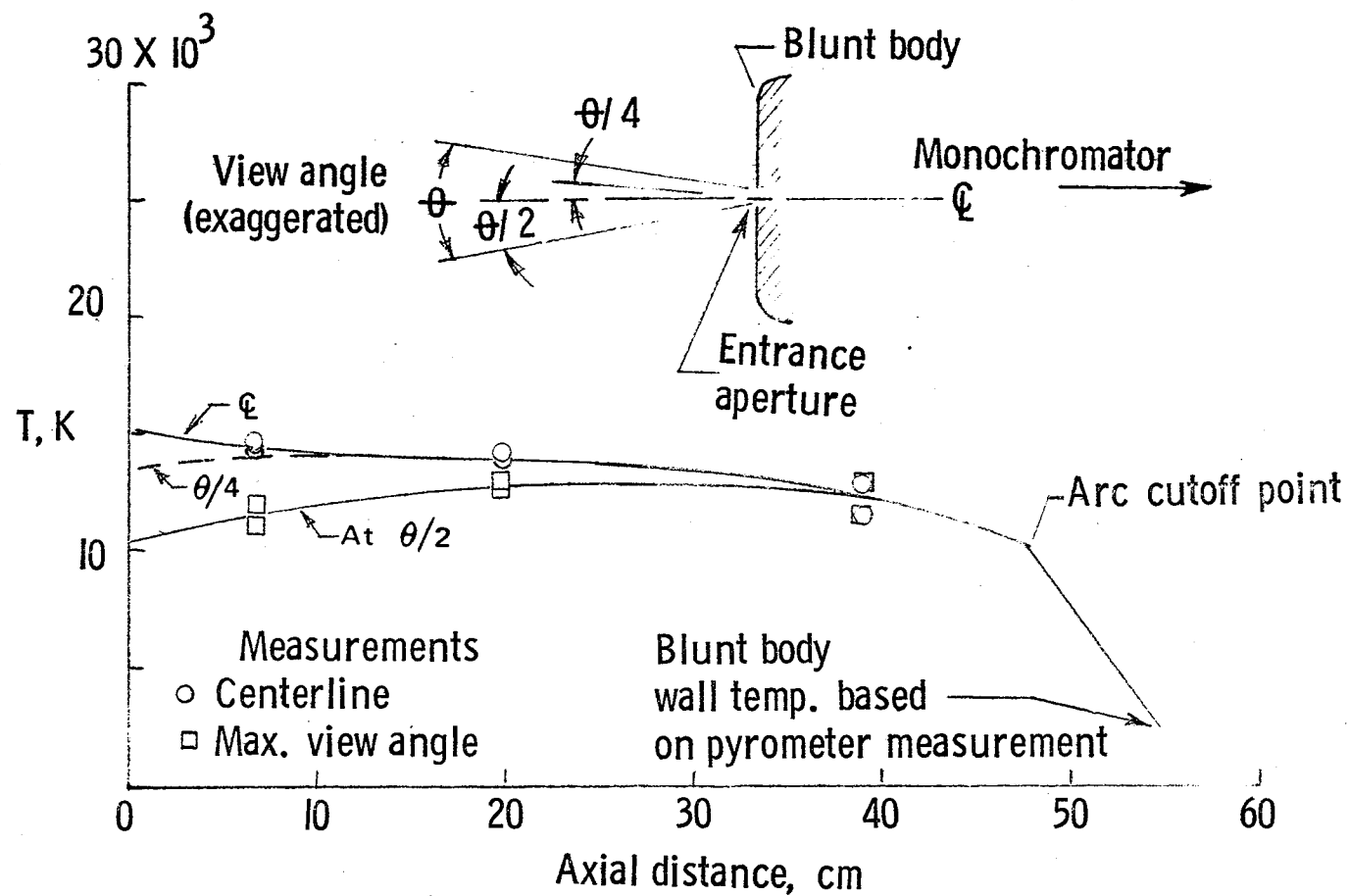
Figure 7.- Axial distribution of pure hydrogen temperature within the field of view of the axial optical system.
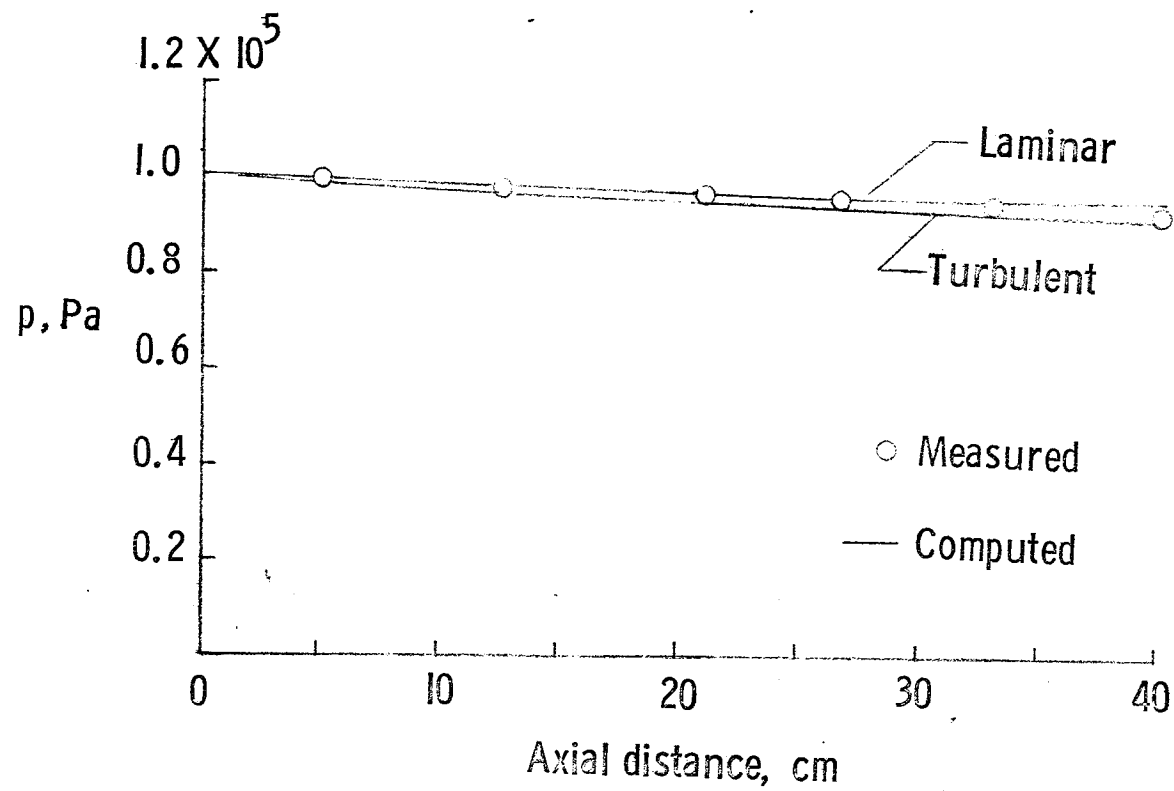
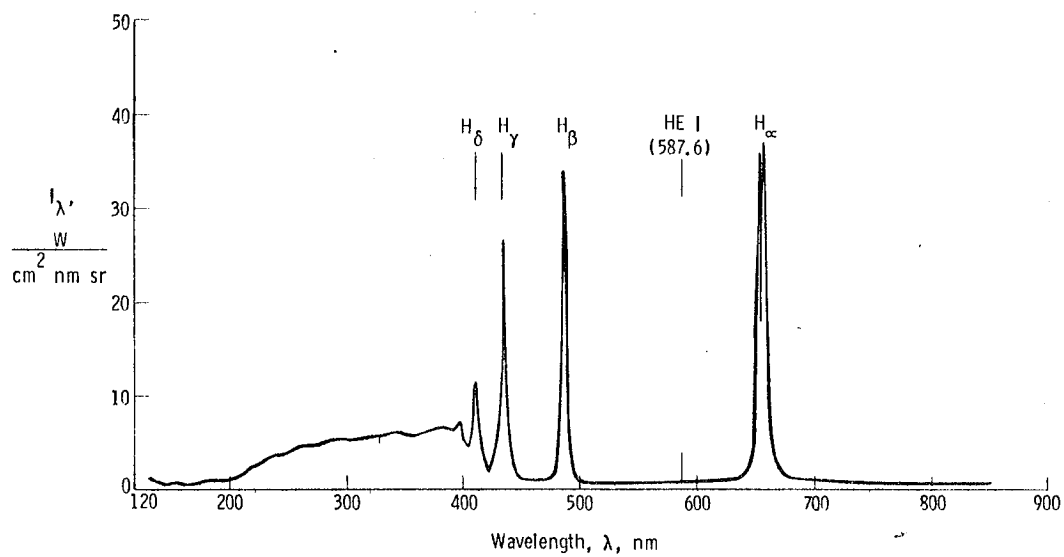Figure 8.- Measured and computed axial pressure distribution for the pure hydrogen case.
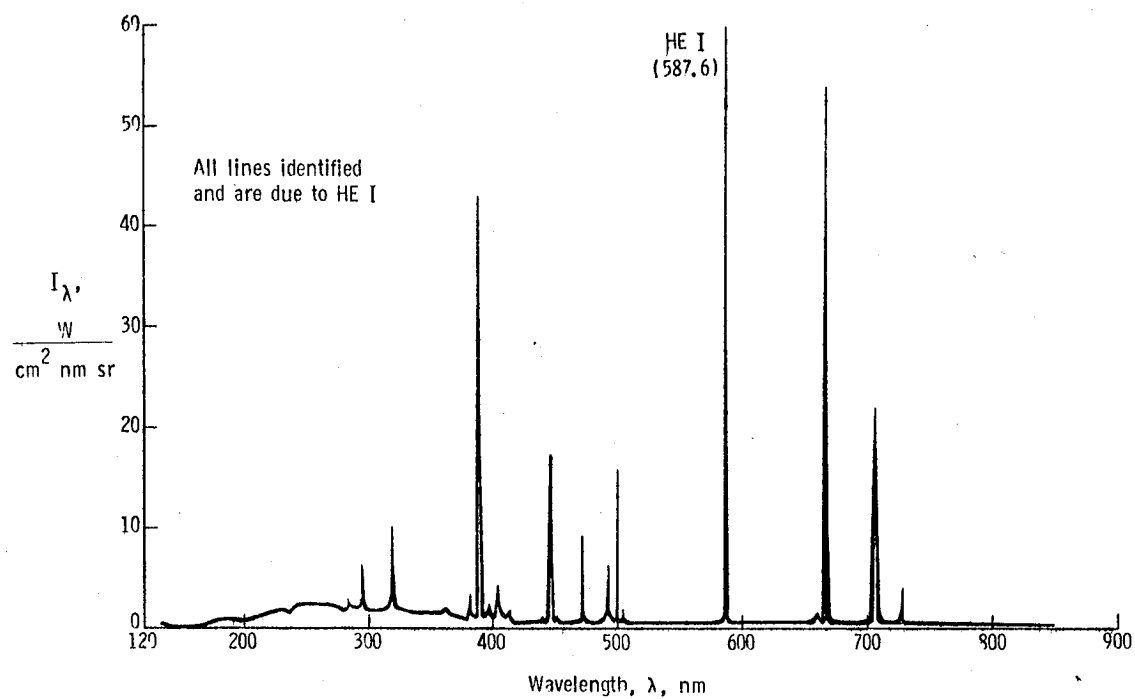
(a) Pure helium.
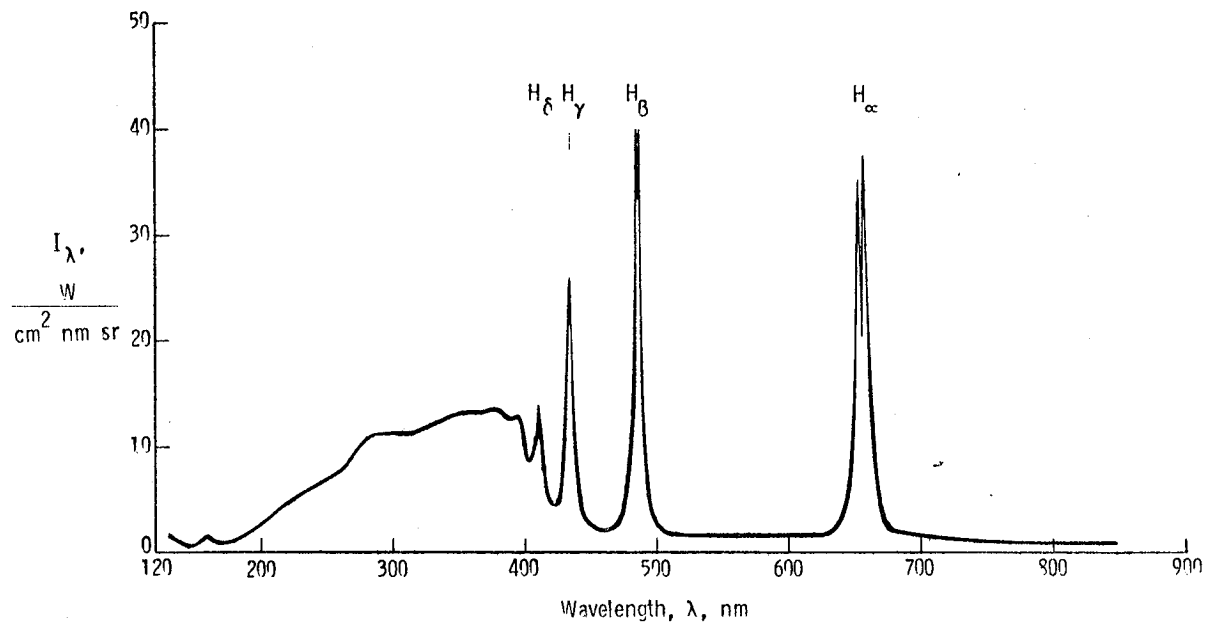
(b) Pure hydrogen.

Figure 9.- Measured spectra for hydrogen, helium, and two mixtures for
arc heater operating at 800 A and 10^5 Pa (1 atm). Wavelength
interval; 130 to 850 nm.
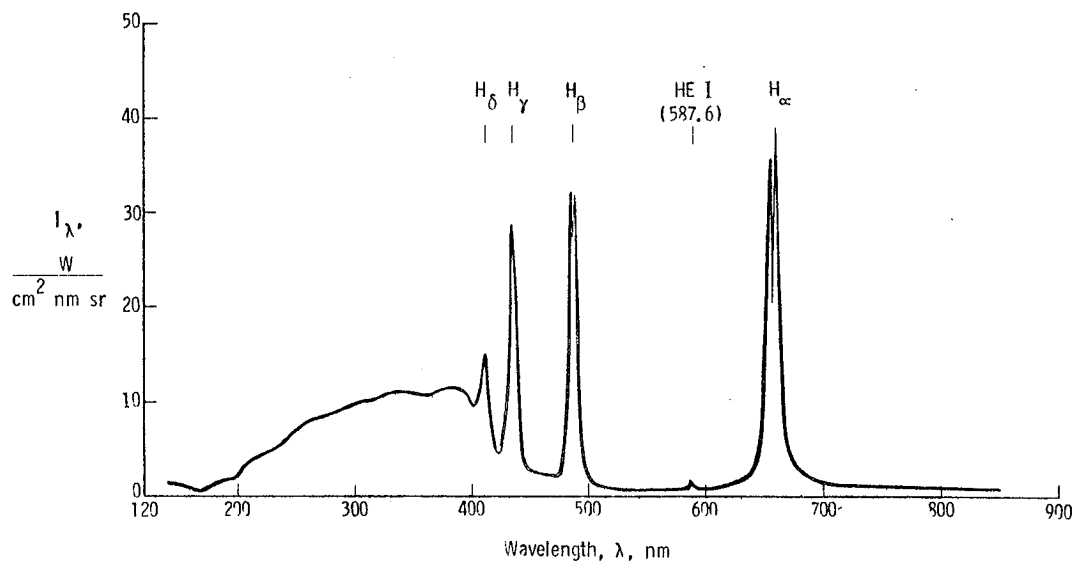
(c)   0.8 hydrogen/0.2 helium by mass.

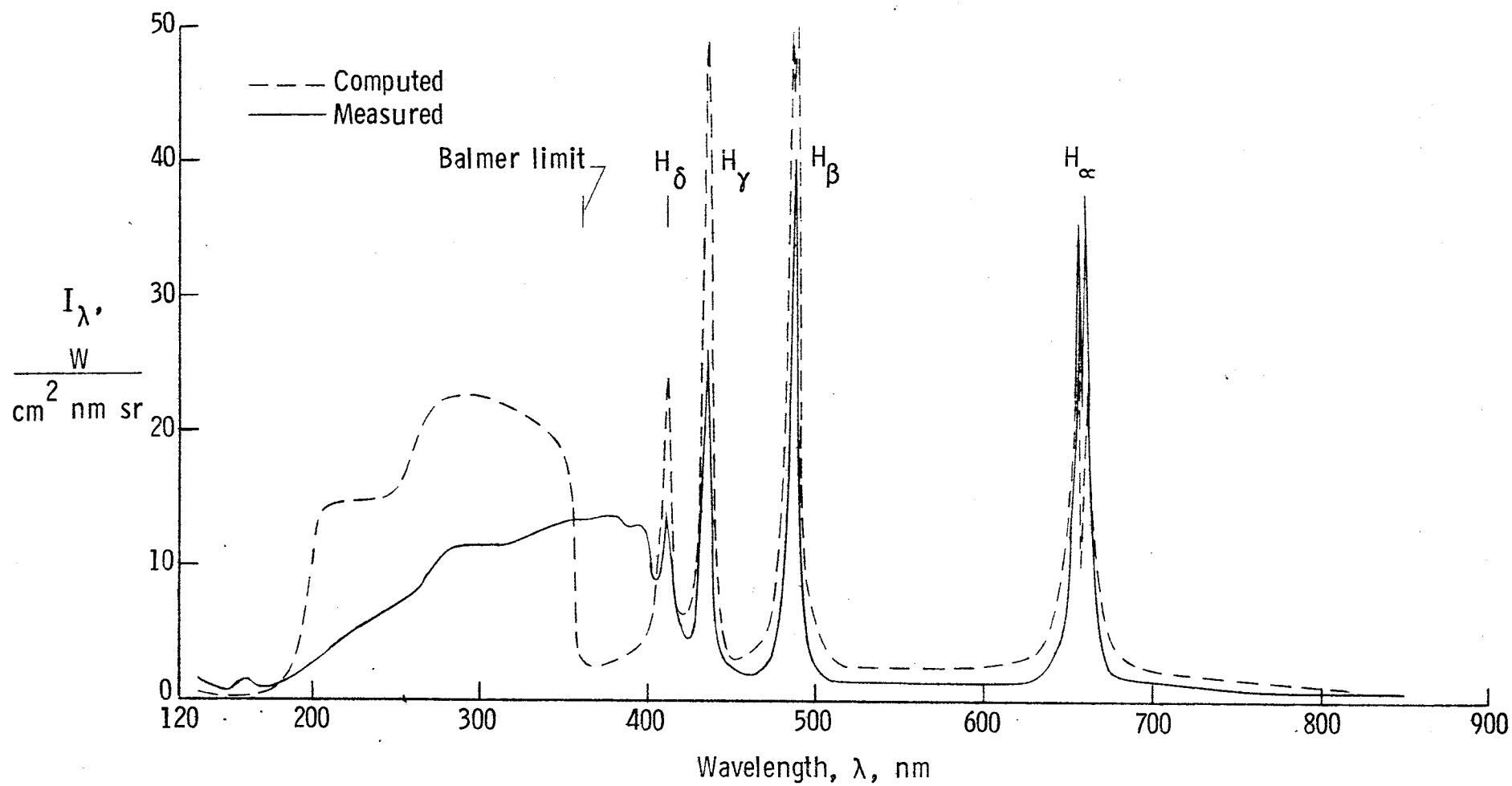(d)   0.2 hydrogen/0.8 helium by mass.

Figure 9.- Concluded.

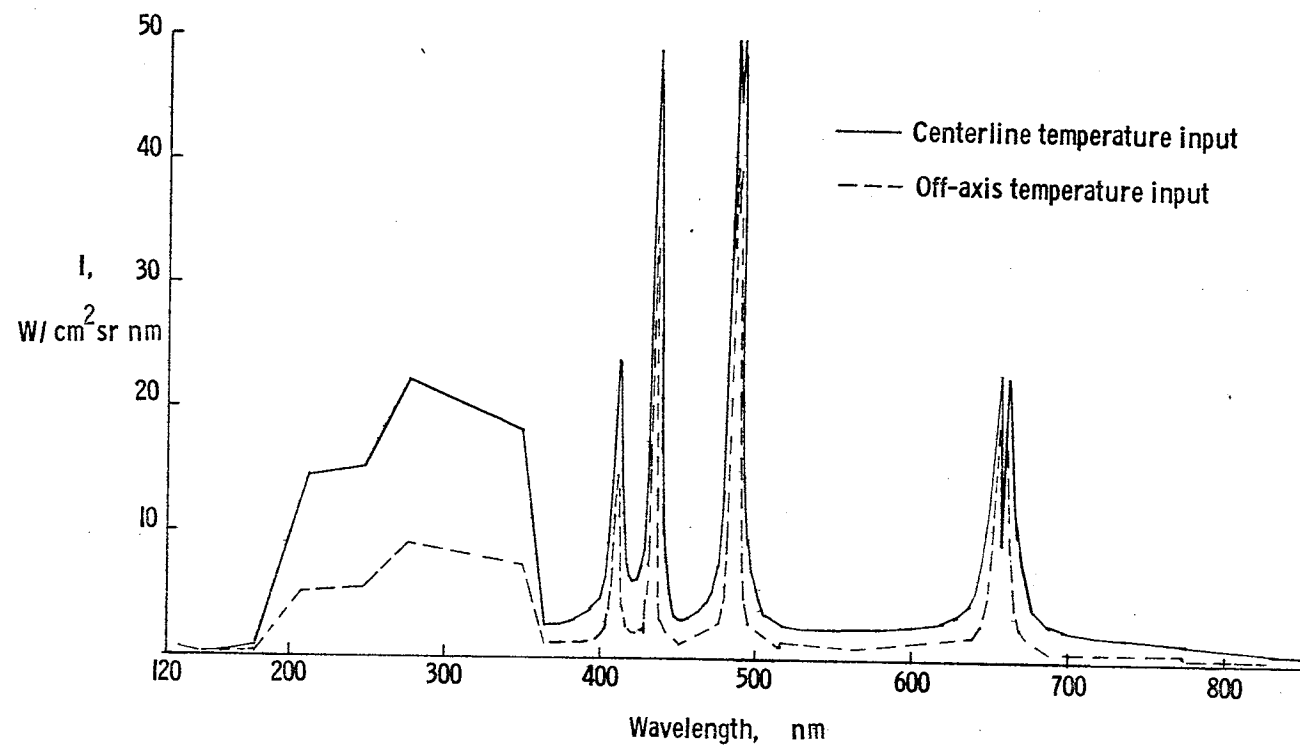Figure 10.- Computed and measured hydrogen spectrum.

Figure 11.- Effect of hydrogen spectrum of radial temperature distribution in the arc heater.
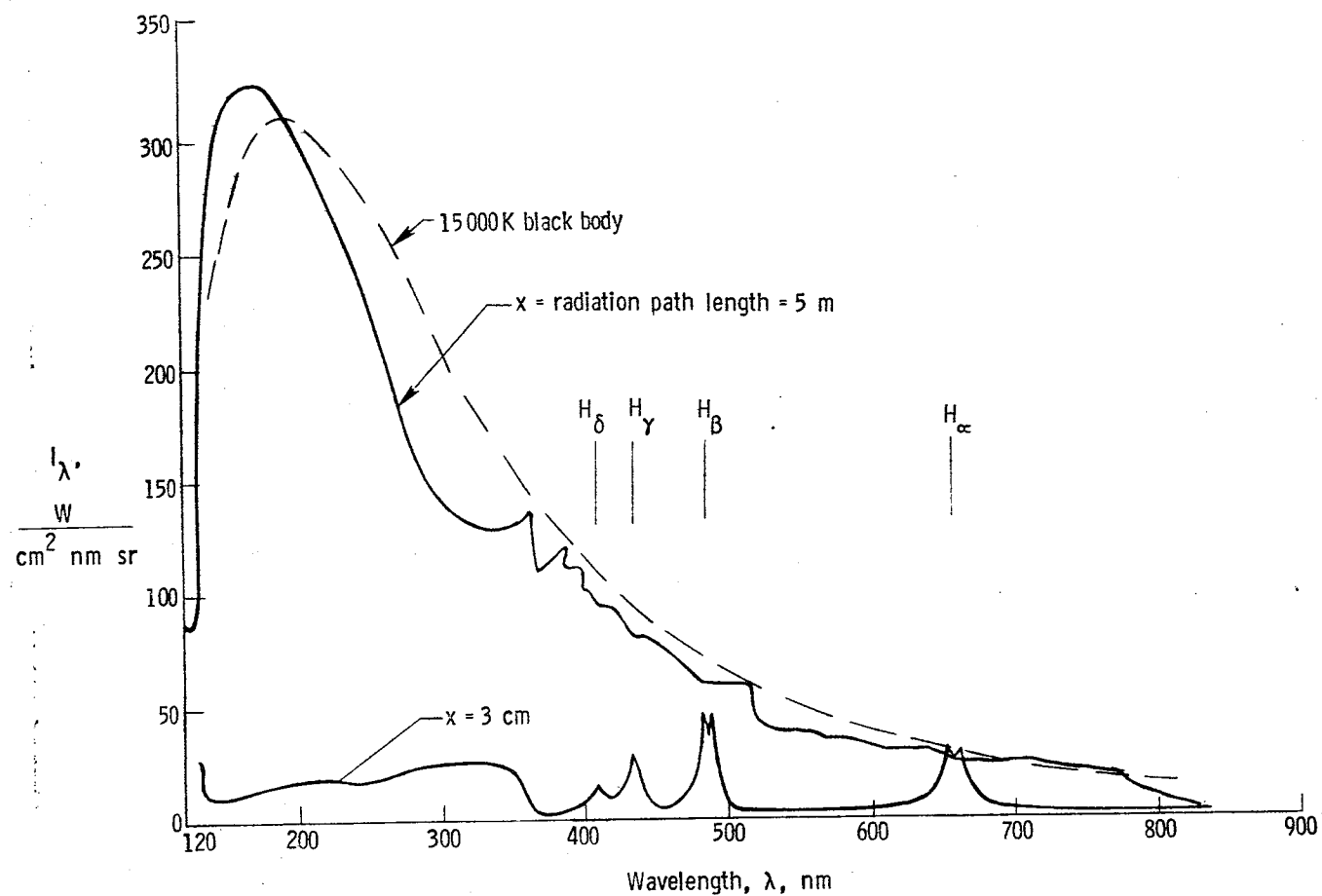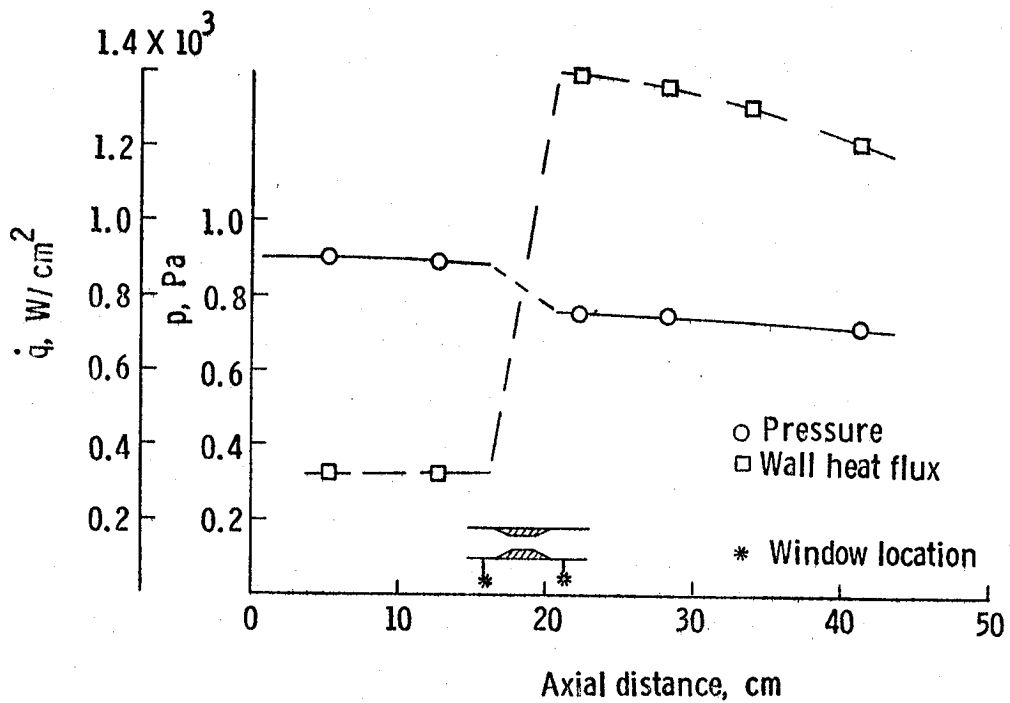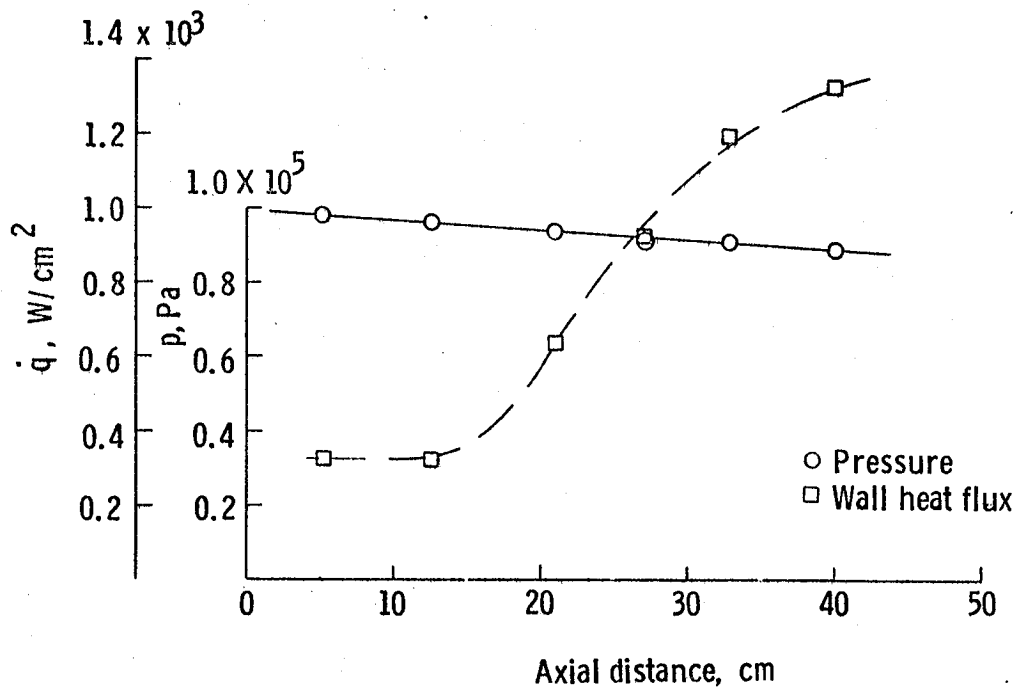
Figure 12.— Computed hydrogen spectrum for 0.5 H_2–0.5 H_e mixture by mass for two different thicknesses of plasma ($14,000$ K $\leq$ T $\leq$ 16,000 K and 5×10^5 Pa $\leq$ p $\leq 6 \times 10^5$ Pa). A 15,000 K black-body curve is shown for reference.

Figure 13.- Carbon-phenolic ablator located in face of blunt body.

Figure 14.- Carbon-phenolic ablator located on arc channel wall.

(a)   With solid ablator mounted on arc channel wall.

(b)   Without solid ablator mounted on arc channel wall.

Figure 15.- Arc heater axial distribution of pressure and wall heat flux.

1. Report No. NASA TM-80192	2. Government Accession No.	3. Recipient's Catalog No.
4. Title and Subtitle Some Experience with Arc-Heater Simulation of Outer Planet Entry Radiation		5. Report Date January 1980
		6. Performing Organization Code
7. Author(s) William L. Wells and Walter L. Snow		8. Performing Organization Report No.
9. Performing Organization Name and Address NASA Langley Research Center Hampton, VA 23665		10. Work Unit No. 506-26-13
		11. Contract or Grant No.
12. Sponsoring Agency Name and Address National Aeronautics and Space Administration Washington, DC 20546		13. Type of Report and Period Covered Technical Memorandum
		14. Army Project No.

15. Supplementary Notes

16. Abstract

An electric arc heater was operated at 800 amperes and 10^5 pa (1 atm) with hydrogen, helium, and two mixtures of hydrogen and helium. A VUV-scanning monochromator was used to record the spectra ($130 \leq \lambda \leq 850$ nm) from an end view while a second spectrometer was used to determine the plasma temperature using hydrogen continuum radiation at 562 nm. Except for pure helium, the plasma temperature was found to be too low to produce significant helium radiation, and the measured spectra were primarily the hydrogen spectra with the highest intensity in the pure hydrogen case. A radiation computer code was used to compute the spectra for comparison to the measurements and to extend the study to simulation of outer planet entry radiation. Conductive cooling prevented ablation of phenolic-carbon material samples mounted inside the arc heater during a cursory attempt to produce radiation absorption by ablation gases.

17. Key Words (Suggested by Author(s)) Outer Planet Entry Radiation Heating Hydrogen/Helium Spactra	18. Distribution Statement Unclassified – Unlimited Subject Category 14,75

19. Security Classif. (of this report) Unclassified	20. Security Classif. (of this page) Unclassified	21. No. of Pages 29	22. Price* $4.50